

# 505. Modeling and experimental validation of a new electromechanical damping device

G. Caruso<sup>1</sup>, O. Ben Mekki<sup>2</sup>, F. Bourquin<sup>3</sup>

<sup>1</sup>ITC-CNR, Area Ricerca CNR, Via Salaria Km 29,300, Monterotondo Stazione (Rome), Italy

<sup>2</sup>Ecole Nationale d'Ingénieurs de Tunis, Laboratoire de Génie Civil (LGC), Tunisia

<sup>3</sup>LCPC-MI, 58, Bd Lefebvre, 75732 Paris Cedex 15, Paris, France

(Received 04 September 2009; accepted 27 November 2009)

**Abstract.** In this paper an innovative passive vibration damping system is proposed, effective on large flexible structures like tall buildings or long-span bridges. It employs an electromechanical actuator composed of a pendulum hinged to the vibrating structure and connected to an electric alternator. Once the pendulum has been tuned on a specific structural eigenmode, like a classical tuned mass damper, vibrational energy can be dissipated or harvested by connecting a resistive electric load to the alternator pins. Some experimental results are presented showing the effectiveness of the device both in vibration control and in energy harvesting.

**Keywords:** Passive vibration control, energy harvesting, electromechanical coupling, tuned mass damper, electrical dissipation.

## 1. Introduction

Classical Tuned Mass Dampers (TMD's) are resonant passive devices able to significantly increase the damping of a structure around a chosen frequency without presenting any instability problem [1]. Various typologies of TMD's have been proposed in the literature, possibly employing also liquid masses (Liquid Tuned Dampers) [2], differing in their mechanical setting, type of damping and design strategy. An important issue concerning the use of TMD's is the optimal choice of the resonance frequency and damping ratio of the device, in order to maximize the vibration damping effect. Different expressions for these parameters have been found in the literature, depending on the type of external excitation and on the objective function chosen in the optimization process. In the case of an undamped structure subjected to an external harmonic excitation over a broad frequency band Den Hartog proposed an optimization method in 1947 [3], aimed at minimizing the maximum of the amplitude of the frequency response function. This optimization method does not apply when damping is present on the primary mass. To this end in [4] a numerical method was proposed to overcome the problem. Analytical expressions for the TMD parameters, valid when damping is present on the primary mass, were proposed in [5], aimed at maximizing the decay of the transient vibrations of the controlled structure. Explicit formulas for the optimal parameters and the effectiveness of a TMD to control structural oscillations caused by more general typologies of external excitations are now well established [2], and several objectives have been pursued in the optimization problem, such as the minimization of the displacement, velocity or acceleration of the primary mass.

---

<sup>1</sup> Corresponding author. E-mail: g.caruso@itc.cnr.it

A well known smart damping device acting much like a classical TMD can be obtained by bonding a piezoelectric patch on a vibrating structure and connecting its electrodes to a shunt electric circuit containing resistive elements [6, 7]. The piezoelectric device converts vibrational energy into electrical energy, which in turn can be dissipated through the resistive impedance. It is useful to damp vibrations of flexible and light structures, e.g. aircraft structures or robot manipulators. Due to its electromechanical coupled properties, this device has also been widely used to harvest energy from ambient vibrations [8, 9].

This issue is receiving great attention in the last years [10]. Energy harvesters are able to extract energy from the ambient and supply it to external users, e.g. wireless sensors for health monitoring of structures, thus avoiding the use of batteries and other power supply devices. Several sources can be considered for energy scavenging. Among the most commonly available sources (e.g. solar, thermal or magnetic) ambient vibrations are of particular interest since they are present in most of all the environments [10, 11, 12].

In this paper an innovative electromechanical actuator is proposed, bearing energy conversion properties similar to the ones of a piezoelectric device, but effective on large structures of civil engineering interest, like tall buildings or long-span bridges. It is composed of a pendulum connected through a shaft and a gear to an electric alternator. The actuator is hinged on the vibrating structure, and the alternator is rigidly connected to the structure itself. While vibrating, the structure put in oscillation the pendulum which, in turn, activates the alternator. Electric energy can be dissipated/harvested by connecting a shunt resistor/battery to the alternator pins. The electromechanical capabilities exhibited by the proposed device can also be exploited to obtain a semi-active vibration control device [13], which can be very effective when the external loading acting on the vibrating structure or the structural characteristics vary in time [14].

In what follows an accurate modelling of the proposed device is presented and used for the design of a vibration control system acting on a bridge mock-up. Both numerical simulations and experimental results are presented, showing vibration damping and energy harvesting capabilities of the proposed device.

## 2. Model of the electromechanical coupled system

It is here considered the modelling of the behaviour of the proposed electromechanical actuator when connected to a vibrating structure. To this end the bridge mock-up reported in Fig. 1a is considered, representing a part of a bridge under construction. The pendulum, represented in Fig. 1b, is hinged to the bridge under one its tips, such to get strong coupling with the in-plane vibrations of the bridge deck around the central pile.

Accordingly the bridge is modelled, employing the classical Euler-Bernoulli beam theory together with the modal reduction technique, as a single degree-of-freedom structure (in-plane vibrations of the bridge deck around the pile), with  $\alpha$  being the relevant modal coordinate. The dynamical behaviour of the structure composed of only the bridge and the pendulum is described by the following equations [13], resembling a one degree-of-freedom system equipped with a standard TMD.

$$\begin{cases} (m^* + m)\ddot{\alpha} + ml\ddot{\theta} \cos \theta - ml\dot{\theta}^2 \sin \theta + c^* \dot{\alpha} + k^* \alpha = f \\ I\ddot{\theta} + ml\ddot{\alpha} \cos \theta + C\dot{\theta} + mgl \sin \theta = 0 \end{cases} \quad (1)$$

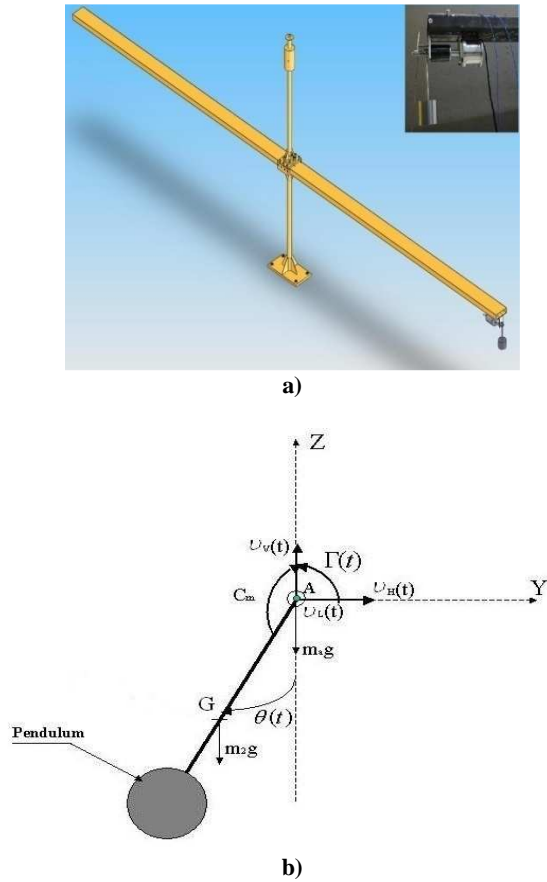


**Fig. 1.** a) bridge mock-up, b) pendulum

In equation (1)  $m^*$  and  $k^*$  are, respectively, the bridge modal mass and stiffness,  $c^*$  is the modal internal damping coefficient,  $f$  is the external transversal load,  $m$  and  $l$  are, respectively, the pendulum mass and length,  $\theta$  is the pendulum rotation angle,  $C$  is the friction coefficient at the hinge,  $I$  is the inertia moment of the pendulum and  $g$  is the gravity acceleration. Moreover, in writing (1), the eigenmode corresponding to the modal coordinate  $\alpha$ , symmetrical with respect to the pile, has been normalized such as to have unitary displacement in correspondence of the deck tips, where both the pendulum and the external force  $f$  are applied; accordingly both  $f$  and the pendulum transversal reaction on the deck coincide with their corresponding modal component. A linearized version of equation (1) is obtained by assuming that  $\theta$  and its time derivative are small, and read as

$$\begin{cases} (m^* + m)\ddot{\alpha} + ml\ddot{\theta} + c^*\dot{\alpha} + k^*\alpha = f \\ I\ddot{\theta} + ml\ddot{\alpha} + C\dot{\theta} + mgl\theta = 0 \end{cases} \quad (2)$$

and is useful in order to evaluate the optimal pendulum length for perfectly tuning the pendulum on the targeted bridge eigenmode. In view of keeping the analysis as simple as possible, the mass of the pendulum is assumed to be lumped at the pendulum tip, in such a

way that  $I=ml^2$ . The reference coupled system (1) can be written in non-dimensional form as follows

$$\begin{cases} (1 + \mu)\ddot{\alpha} + \sqrt{\mu}\ddot{\Theta} + 2\xi\dot{\alpha} + \alpha = \frac{f}{m^*} \\ \ddot{\Theta} + \sqrt{\mu}\ddot{\alpha} + 2\zeta p\dot{\Theta} + p^2\Theta = 0 \end{cases} \quad (3)$$

with

$$\begin{cases} \omega^* = \sqrt{\frac{k^*}{m^*}}, & \omega = \sqrt{\frac{g}{l}}, & \mu = \frac{m}{m^*}, & \tau = \omega^* t, & \dot{\Theta} = \frac{d\Theta}{d\tau} \\ \Theta = \sqrt{\frac{m}{m^*}}\theta, & p = \frac{\omega}{\omega^*}, & \zeta = \frac{C}{2ml^2\omega}, & \xi = \frac{c^*}{2m^*\omega^*} \end{cases} \quad (4)$$

For harmonic excitation and neglecting the internal damping of the structure, the optimal tuning parameter  $p$  and the optimal damping coefficient  $\zeta$  are given, according to Den Hartog formulation [3], by

$$\begin{cases} p^{opt} = \frac{1}{1 + \mu} \\ \zeta^{opt} = \sqrt{\frac{3\mu}{8(1 + \mu)}} \end{cases} \quad (5)$$

It is now considered the presence of the alternator, bonded under the bridge deck and coupled to the pendulum by means of a shaft and a gear of reduction ratio  $\beta$ . The alternator contains three coils and thus, when the shaft is rotating, it behaves like a triphase generator and an electric voltage is induced between each coil and the neuter, with phase shift equal to  $120^\circ$  between each couple of phases. In order to add an electrical damping, three equal resistive loads of resistance  $R$  are applied to the three alternator pins and connected together in a star configuration, like shown in Fig. 2.

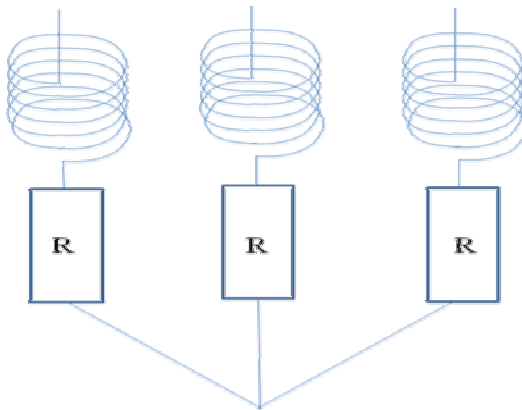


**Fig. 2.** Electrical scheme of the alternator connected to a resistive load

In order to describe the effect of the alternator on the system dynamics, the new unknown  $i = -\dot{q}$ , equal to the electric current flowing into each resistive load, must be introduced, being  $q$  the total displaced electric charge in each phase at time  $t$ . Due to the electromechanical coupling yielded by the alternator, equation (1)<sub>2</sub> must be replaced with

$$I\ddot{\theta} + ml\ddot{\alpha} \cos\theta + C\dot{\theta} + mgl \sin\theta + \beta k_c i \sin(\beta\theta) = 0 \quad (6)$$

and the following equation relevant to the electric equilibrium of each of the three circuits connected to the alternator pins must be also considered

$$L_e \ddot{q} + (r + R)\dot{q} = k_e \beta \dot{\theta} \sin(\beta\theta) \quad (7)$$

In (6) and (7) the last term is due to the contribution of the alternator, which couples together the mechanical equilibrium equation relevant to the pendulum and the electric equilibrium equation relevant to the circuit connected to the alternator pins. In particular,  $k_c$  and  $k_e$  are constant parameters relevant to the alternator. The term proportional to  $k_c$ , appearing in (3), is the mechanical couple exerted by the electromagnetic field inside the alternator on the rotating shaft when a current  $i$  is circulating in the alternator coils. The term proportional to  $k_e$ , appearing in (4), is the difference of electric potential induced between the alternator coil pin and the neuter by the variation of magnetic flux due to a rotation of the shaft with angular velocity  $\dot{\theta}$ . Moreover,  $L_e$  is the inductance of each coil and  $r$  is its internal resistance.

It turns out that the inductive voltage drop  $L_e \ddot{q}$  in (7) is negligible with respect to the other terms, so from equation (7) it is possible to evaluate  $i = -\dot{q}$  and substitute it into equation (6) obtaining

$$I\ddot{\theta} + ml\ddot{\alpha} \cos\theta + C_{eq} \dot{\theta} + mgl \sin\theta = 0 \quad (8)$$

where

$$C_{eq} = C + \frac{\beta^2 k_e k_c}{r + R} \sin^2(\beta\theta) \quad (9)$$

Equations (8-9) show that the effect of the alternator connected to a resistive load is to add damping to the structure. The added damping term is not constant in time but it is modulated by the sinusoidal nonlinear term  $\sin^2(\beta\theta)$ , due to the constitutive behaviour of the alternator. This prevents from the use of the classical TMD optimization formulas for the evaluation of the optimal value of  $R$ . The system behaviour is shown in the next section by integrating the nonlinear system (10) in the case of harmonic excitation.

$$\begin{cases} (m^* + m)\ddot{\alpha} + ml\ddot{\theta} \cos\theta - ml\dot{\theta}^2 \sin\theta + c^* \dot{\alpha} + k^* \alpha = f \\ I\ddot{\theta} + ml\ddot{\alpha} \cos\theta + C\dot{\theta} + mgl \sin\theta = \beta k_c \dot{q} \sin(\beta\theta) \\ L_e \ddot{q} + (r + R)\dot{q} = k_e \beta \dot{\theta} \sin(\beta\theta) \end{cases} \quad (10)$$

### 3. Passive vibration control and energy harvesting under harmonic excitation

In this section the nonlinear system (10) is numerically integrated, subjected to an harmonic external excitation  $f = A \cos(\overline{\omega}t)$ . To this end, the structural parameters given in table 1 are employed, relevant to the bridge mock-up used in the experiments described in the next section.

**Table 1.** Parameters relevant to the bridge mock-up used for the experimental validation of the proposed electromechanical actuator

$m$ kg	$m^*$ kg	$I$ kg m <sup>2</sup>	$l$ m	$k^*$ N/m	$c^*$ Ns/m	$C$ Ns/m	$k_c$ N/A	$K_e$ Ns/m	$\beta$	$r$ $\Omega$	$L_a$ H
2.85	25.90	0.1430	0.224	1332	0.029	0.035	0.3	0.04	10	0.85	0.0036

Both the “ode15s” matlab solver and a Newmark scheme have been employed for the numerical integration, giving similar results. Since the system is nonlinear, it is not possible to directly compute the frequency response function. When the harmonic load is applied to the structure, after a brief transitory period, the system reaches a periodic regime and the modal coordinate  $\alpha$  exhibits a sinusoidal behaviour. In Fig. 3 the amplitude of  $\alpha$  is reported as a function of the excitation frequency, normalized with respect to the excitation force amplitude. Several values of resistance  $R$  are used in the numerical simulations such as to show its influence on the achieved damping. The curves resemble the ones relevant to a classical TMD. In particular for small values of resistance only a single peak in the frequency response is visible whereas, for larger values of resistance, two peaks appear, similarly to the behaviour of a classical TMD when large values or small values of viscous damping are employed, respectively. As a matter of fact, small values of  $R$  imply a large electromagnetic force exerted by the magnetic fields on the rotating shaft whereas large values of  $R$  imply small values of circulating currents, i.e. small electromagnetic forces. In particular, the open circuit condition is equivalent to an infinite value of resistance whereas the short circuit condition implies the presence of the only internal resistance  $r$ , which cannot be further reduced. The optimal value of resistance, minimizing the maximum of the amplitude curves, turns out to be close to  $1\Omega$ .

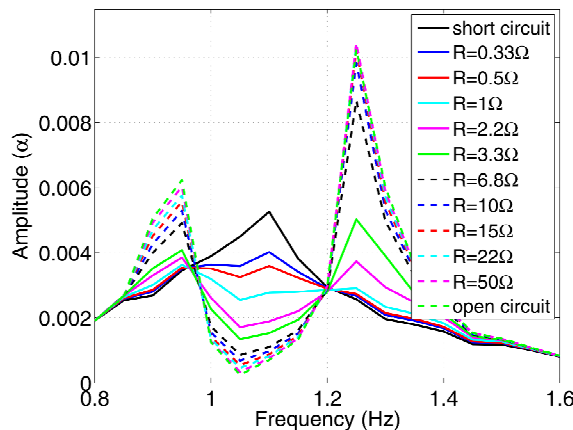


**Fig. 3.** Numerical simulations: normalized amplitude of the modal coordinate  $\alpha$  versus excitation frequency. Several values of resistance  $R$  are tested

#### 4. Energy harvesting issues

Energy harvesting issues are here explored, and the theoretical electric power  $P$  extracted from the vibrating system, equal to  $Ri^2$ , is computed. Since  $i$  is not constant in time, a time averaged value  $\bar{P}$  of the power is evaluated according to the following expression

$$\bar{P} = \frac{1}{t_2 - t_1} \int_{t_1}^{t_2} Ri^2 dt \quad (11)$$

where  $t_1$  is chosen large enough such as the periodic regime of the solution has been reached and  $t_2 - t_1$  is large enough such as to include several complete periods; in principle, in the simulations, it would be enough to choose  $t_2 - t_1$  equal to a single period, since the solution is in periodic regime, but in the experiments showed in the next section it is convenient to average the extracted power over many periods to reduce noise effects. The averaged extracted power, normalized by the squared of the excitation force amplitude, is reported in Fig. 4 versus the excitation frequency. The squared of the force amplitude is chosen as normalization factor since the power is proportional to the square of  $i$ . Several values of the electric resistance are investigated to study the effect of the electric load applied to the alternator on the amount of power harvested. The curves relevant to short circuit and open circuit conditions are identically equal to 0 since no electric load is applied to the alternator pins and, hence, no power can be extracted. For small values of resistance the maximum power is extracted at a frequency close to the central peak in the frequency response appearing at low resistance values whereas, for large values of resistance, the maximum power is extracted at frequencies close to the two peaks exhibited by the frequency response curve when large resistances are employed. A value of resistance close to  $1\Omega$  maximizes the electric power extracted at the central resonance whereas a value of resistance close to  $6.8\Omega$  maximizes the power extracted at the two external peak frequencies. Further increasing the value of resistance above  $6.8\Omega$  yields a lower amount of extracted power, becoming negligible for very large values of resistance.

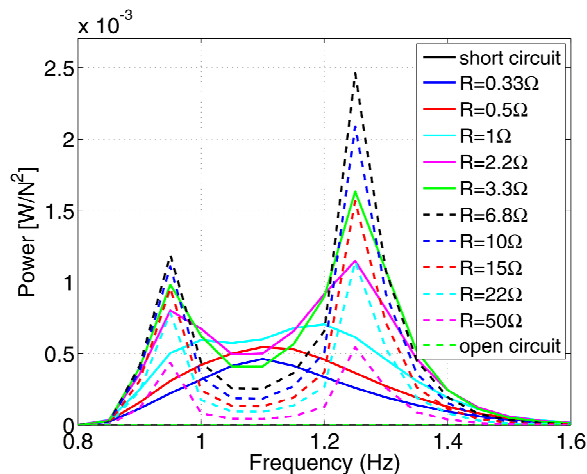


**Fig. 4.** Numerical simulations: normalized power harvested versus excitation frequency. Several values of resistance  $R$  are tested

## 5. Experimental results

In this section some experimental results are presented concerning the passive damping of the bridge mock-up shown in Fig. 5a. The structure is made of steel (Young modulus  $E=210$  GPa, Poisson ratio  $\nu=0.3$  and mass density  $\rho=7850$  kg/m<sup>3</sup>) and is composed of

- A lower cylindrical tube of outer diameter 45 mm, thickness 2 mm and height 1035 mm.
- An upper cylindrical bar of diameter 45 mm and height 1215 mm.
- A hollow beam of dimensions 150 mm x 50 mm x 3 mm and length 6 m.
- A basis plate of dimensions 22 mm x 40 mm x 15 mm.



**Fig. 5.** Experimental setup: a) bridge mock-up equipped with pendulum-alternator actuator and eccentric mass shaker, b) detailed view of the pendulum-alternator actuator

The mock-up is equipped with the pendulum-alternator actuator previously described shown in Fig. 5b, connected at one of the bridge deck ends. The pendulum length has been optimally chosen in order to tune the pendulum on the first torsional eigenmode of the structure, at frequency 1.14Hz. The structure has been harmonically excited by using an eccentric mass shaker, visible on right side of Fig. 5a, with mass  $m_s$  equal to 2kg and eccentricity  $e$  equal to 6cm. The shaker provides a known sinusoidal transversal force component, equal to  $m_s \bar{\omega}^2 e \sin(\bar{\omega}t)$  being  $\bar{\omega}$  the angular speed of the shaker, which is able to excite the considered eigenmode. The frequency of the shaker could be varied by changing the feeding voltage and the actual excitation frequency has been measured in real time by using an electromagnetic sensor. Three equal resistances  $R$  have been connected to the alternator pins in star configuration, as previously shown in Fig. 2, in order to achieve vibration damping or to measure the harvestable energy. The structural vibrations induced by the shaker have been measured by using an accelerometer bonded on the bridge-deck tip, visible in Fig 5b. In order to estimate the harvested electric power the difference of potential at the pins of one of the three resistors connected to the alternator has been measured as well. All the sensors signals have been acquired using a data acquisition card and a MatLab-Simulink program. The modal coordinate  $\alpha$  has then been estimated by dividing the accelerometer signal, after periodic regime condition was reached, by  $\bar{\omega}^2$  and normalizing with respect to the excitation force amplitude. The obtained experimental curves are reported in Fig. 6, relevant to different values of resistance  $R$ .

The experimental curves well reproduce all the features described in the previous section, relevant to the corresponding simulation results reported in Fig. 3. In particular the two external peaks are visible together with the central resonance peak reached under short

circuit condition. The peak disposition is slightly different from the one in Fig. 3 since it is difficult to reach a perfect tuning condition of the pendulum during experiments. Differences in absolute values between experimental and theoretical results may depend on the calibration of the sensor used in the experimental setup, and do not constitute a problem.

An optimal value of resistance equal to  $1\Omega$  was experimentally determined, able to minimize the maximum of the amplitude of  $\alpha$ ; this value perfectly coincides with the corresponding optimal theoretical resistance found in the previous section.

Finally, in Fig. 7 the average extracted power is reported, normalized by the square of the excitation force amplitude. The experimental power has been determined by performing the integration in formula (11), where the integrand function has been now equivalently chosen as  $V^2/R$ , being  $V$  the difference of electric potential measured across one of the external resistance pins. The behaviour of the curves in Fig. 7 closely resembles the corresponding theoretical behaviour reported in Fig. 4. The experimentally determined values of resistance able to extract the largest amount of electric power at the central and external resonance peaks are, respectively, equal to  $1\Omega$  and  $3.3\Omega$ . The first one coincides with the corresponding theoretical one whereas the second one is slightly lower than the corresponding theoretical value.

These experimental results validate the proposed model describing the dynamical behaviour of a bridge mock-up equipped with the electromechanical actuator, confirming the ability of the control device on both vibration damping and energy harvesting.

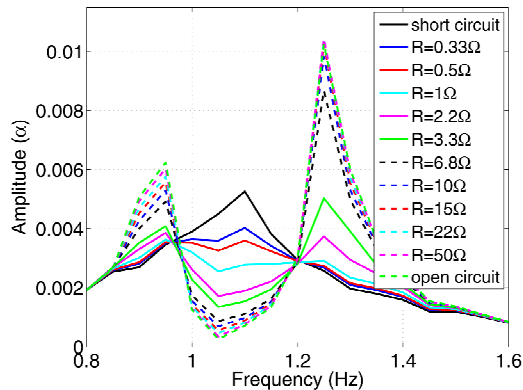


**Fig. 6.** Experimental results: normalized amplitude of the modal coordinate  $\alpha$  versus excitation frequency. Several values of resistance  $R$  are tested

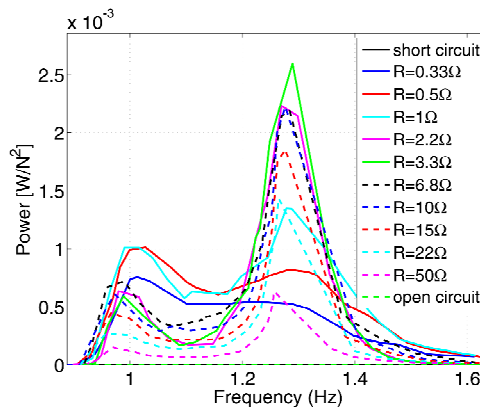


**Fig. 7.** Experimental results: normalized power harvested versus excitation frequency. Several values of resistance  $R$  are investigated

## 6. Conclusions

A new electromechanical actuator was presented in this paper, composed of a pendulum connected to an electric alternator. It has the ability to convert vibrational energy into electric energy, which can be easily dissipated into an electric resistance by Joule effect. This property is similar to the one relevant to the very well known piezoelectric damping devices, useful in the case of light and flexible structure. On the contrary, the proposed actuator can be effective on large structures, like tall buildings and bridges. Due to the electric conversion operated by the alternator, the proposed device can be used also for energy harvesting purposes, which is a very promising area for the many technological applications. A theoretical model accurately describing the nonlinear behavior of the proposed device was presented in this paper and the main features exhibited by the numerical simulations were discussed as well. Finally, some experimental results were presented, obtained on a bridge mock-up representing a bridge under construction. The experimental results were in good agreement with the theoretical predictions and confirmed the ability of the proposed actuator to be used both as a vibration damping and an energy harvesting device.

## References

- [1] Housner G. W., Bergman L. A., Caughey T. A., Chassiakos A. G., Claus R. O., Masri S. F., Skelton R.E., Soong T. T., Spencer B. F., Yao J. T. P. Special Issue: structural control: past, present and future. *Journal of Engineering Mechanics ASCE*, 1997, 123(9), 897-971.
- [2] Soong T. T., Dargush G. F. *Passive Energy Dissipation Systems in Structural Engineering*. Wiley Sons, 1997.
- [3] Den Hartog J. P. *Mechanical Vibrations*. New York: McGraw Hill Book Co., 1947.
- [4] Thomson A. G. Optimum tuning and damping of a dynamic vibration absorber applied to a force excited and damped primary system. *Journal of Sound and Vibration*, 1981, 77(3), 403-415.
- [5] Fujino Y., Masato A. Design formulas for tuned mass dampers based on a perturbation technique. *Earthquake Engineering and Structural Dynamics*, 1993, 22, 833-854.
- [6] Hagood N. W., Von Flotow A. Damping of Structural Vibrations with Piezoelectric Materials and Passive Electrical Networks. *Journal of Sound and Vibration*, 1991, 146(2), 243-268.
- [7] Caruso G. A critical analysis of electric shunt circuits employed in piezoelectric passive vibration damping. *Smart Materials and Structures*, 2001, 10, 1059-1068.
- [8] Liao Y., Sodano H. A. Model of a single mode energy harvester and properties for optimal power generation. *Smart Materials and Structures*, 2008, 17.
- [9] Renno J. M., Daqaq M. F., Inman D. J. On the optimal energy harvesting from a vibrating source. *Journal of Sound and Vibration*, 2008, 320, 386-405.
- [10] Anton, S. R., Sodano, H. A. A review of power harvesting using piezoelectric materials (2003-2006). *Smart Materials and Structures*, 2007, 16.
- [11] Sodano H. A., Inman D. J., Park G. A review of power harvesting from vibration using piezoelectric materials. *Shock and Vibration Digest*, 2004, 36(3), 197-205.
- [12] Stephen N.G. On energy harvesting from ambient vibration. *Journal of Sound and Vibration*, 2005, 293, 409-425.
- [13] Ben Mekki O., Bourquin F., Maceri F., Nguyen Van Phu C. An adaptive pendulum for evolving structures. *Structural Control and Health Monitoring*, in press.
- [14] Symans M. D., Constantinou M. C. Semi-active control systems for seismic protection of structures: a state-of-the-art review. *Engineering Structures*, 1999, 21, 469-487.